

## Optimization of plates reinforced with different initial slope and variable number of carbon fibers

Eduardo da Rosa Vieira<sup>a,b\*</sup> , Daniel Milbrath de Leon<sup>b</sup> , Rogério José Marczak<sup>b</sup> 

<sup>a</sup> Federal Institute of Rio Grande do Sul – IFRS, Campus Rio Grande, Rio Grande, RS, Brazil. Email: [vieira.r.eduardo@hotmail.com](mailto:vieira.r.eduardo@hotmail.com)

<sup>b</sup> Federal University of Rio Grande do Sul – UFRGS, Department of Mechanical Engineering, Porto Alegre, RS, Brazil. Email: [daniel.leon@ufrgs.br](mailto:daniel.leon@ufrgs.br), [rato@mecanica.ufrgs.br](mailto:rato@mecanica.ufrgs.br)

\* Corresponding author

<https://doi.org/10.1590/1679-78257584>

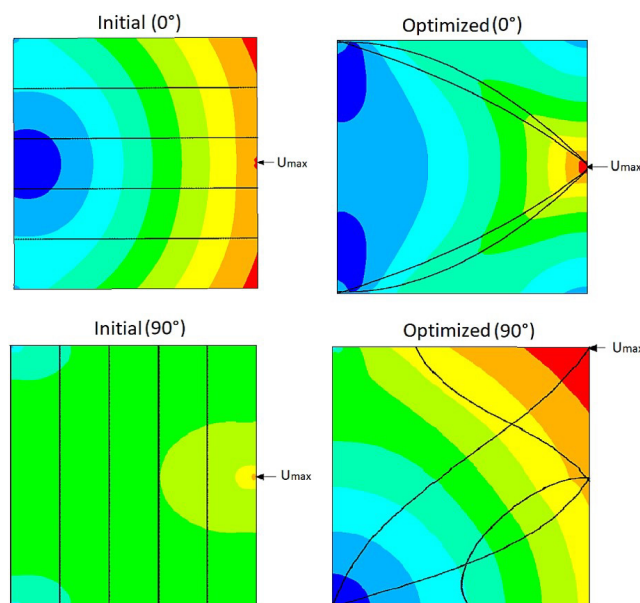
### Abstract

Optimization methods for curvilinear reinforcements placement aims to improve mechanical response of structure. Whenever a gradient-based method is used to optimization, it is necessary arbitrate an initial placement for the fibers. This initial guess has influence on the result. This work aims to observe the influence of the initial positioning of straight carbon fiber in epoxy resin plates, which had their compliance minimized by Sequential Linear Programming. The maximum displacement is observed too, even if it is not an objective function. The case studies were carried out on the same structure and the number of fibers and its slope were changed. Variation of the force slope was also evaluated. The results confirmed an influence of the initial slope in results. The addition of a greater number of fibers does not always cause a better performance in the design. To achieve the best results, it is essential that the initial arrangement be configured in such a way as to provide proximity of the ends of the fibers and the forces and supports. It's important to try to place the fibers with axial directions close to the axial direction of the force.

### Keywords

Composite Optimization, Reinforced Plates, Sequential Linear Programming, CRFP, VSC.

### Graphical Abstract



Received: March 17, 2023. In revised form: June 24, 2023. Accepted: June 27, 2023. Available online: June 28, 2023

<https://doi.org/10.1590/1679-78257584>



Latin American Journal of Solids and Structures. ISSN 1679-7825. Copyright © 2023. This is an Open Access article distributed under the terms of the [Creative Commons Attribution License](https://creativecommons.org/licenses/by/4.0/), which permits unrestricted use, distribution, and reproduction in any medium, provided the original work is properly cited.

## 1 INTRODUCTION

The improvement of mechanical projects is related to the implementation of new materials applied in their design. In this way, the improvement of materials makes it possible for more efficient structures to be developed and applied in the high-tech industry (Vasiliev and Morozov, 2007). Nowadays, there is a gradual replacement of metallic materials by composites with high performance which demonstrate several advantages in relation to traditional metallic parts. One of the main aspects is the excellent mechanical performance associated with the low weight, which significantly reduces energy consumption for the operation of machines (Bai, 2013; Rana and Figueiro, 2016).

Among these materials, fiber-reinforced composites stand out, especially carbon fibers, which associated with polymer matrices form a class called CFRP (Carbon Fiber-Reinforced Polymers). CRFPs, in addition to having high stiffness, develop an excellent ratio between weight and mechanical strength, good adhesion between fibers and matrix, low rates of corrosion and creep, and a high number of cycles to fatigue failure (Aragh et al, 2021; Wu, Raju, Weaver, 2018). In traditional applications, these materials maintained a regular positioning, with straight and equidistant reinforcements. However, the development of manufacturing techniques that allowed the manufacture of curvilinear filaments, which could be used as reinforcements in composites, enabled an even greater advance in the evolution of these materials (Albazzan, et al., 2019).

These techniques had commercial application from the 1980s, and among them, Automated Fiber Placement (AFP) stands out, which despite not being the first method developed, was the first to popularize the manufacturing of these materials. Although quite effective, the AFP has serious manufacturing limitations that, when not respected, produce parts with defects, which often compromise structural performance. In this way, other methods were being developed, such as Continuous Tow Sharing (CTS), Additive Manufacturing (AM) and Tailored Fiber Placement (TFP). These methods severely reduced fabrication limitations, allowing the design of more complex structures with high reliability, reproducibility and low raw material waste (Punera and Mukherjee, 2022). So, the parts manufactured by these techniques and implementing variable reinforcements formed a class called Variable Stiffness Composites (VSC), which have different stiffness along the structures. In addition to the VCS, the concept of VAT (Variable Angle Tow) was defined, which are composed of layers in which there is freedom for individual variation of the path of each reinforcement (Kesarwani, 2017; Brooks and Martins, 2018).

The association of the VSC with optimization methods allowed a significant evolution of the materials, since by changing the positioning and orientation of the reinforcements, it is possible to maximize the capacity of each structure in each specific application. In this way, unique parts can be designed and built, bringing together the best of each material for the exact requirement of each mechanical system (Nikbakt et al., 2018). Thus, high-tech industries – such as aerospace and automotive – already employ parts manufactured in CRFP and designed using optimization. In most cases, the optimization emphasis is on increasing stiffness, reducing strain and improving stress distribution, avoiding concentration points (Das et al., 2021; Meng et al., 2020).

Several factors influence the performance of VSC, such as material thickness, layer stacking sequence, filament morphology and others. However, it should be noted that the orientation of the reinforcements is one of the main factors in their mechanical properties. Thus, the implementation of mathematical optimization methods to obtain the best positioning of the reinforcements is an excellent solution in the search for better structures (Jiang et al., 2008; Monte et al., 2017). To carry out the optimization of the project, the employed techniques can either be based on the gradient of the function or heuristic methods. Function gradient-based methods can be linear or non-linear, and for each of these groups, there are a number of techniques that can be successfully implemented. One of the linear techniques with high applicability is Linear Programming (LP). From an initial positioning of the variables, it uses the objective function and its gradient at the point to obtain the optimum. In turn, the implementation of Sequential Linear Programming (SLP) is the consecutive use of this technique until a stopping criterion is reached. Thus, in SLP the optimization cycles are repeated in order to reach a global minimum or a good local minimum (Arora, 2016; Kochenderfer and Wheeler, 2019). Linked to the SLP, it is common that both the Finite Difference Method (FDM) and the Moving Limits are implemented. The MFD searches for an approximation of the function gradient at the point through an infinitesimal perturbation on a design variable. In general, it is applied in cases where there is not enough information to calculate the derivative at the point or this calculation is too complex. Moving Limits are used to reduce the processing time in SLP, since they can change their dimensions as the algorithm approaches a local or global minimum. Thus, reducing the search space as the optimization process converges to a minimum point or expanding this space if it is moving away from a minimum point (Nocedal and Wright, 2006).

It should be noted that, for reinforcement optimization problems, there are two ways of establishing the design variables. The first one is based on discretizing the entire structure and defining the angles of the structure's elements

as design variables. Thereby, from obtaining the optimal orientations of the elements, the path in which the fibers will be implemented is established. However, the total body discretization develops a large number of design variables, making the process computationally slow (Van Tooren and Elham, 2016). The second way to perform the optimization is to establish mathematical curves that represent the reinforcements. Although this situation reduces the search space when compared to the total discretization of the structure, the design variables are the positioning and orientation of these curves, which reduces the computational time (Abdalla et al., 2009).

In an initial work, linear curves were established with only one design variable. In this case, a curve was implemented and the other curves were parallel to it (Gürdal and Olmedo, 1993). In sequence, using a linear curve, an additional axis system was implemented, which provided greater freedom for the optimization of the filaments and more interesting results were achieved (Gürdal et al., 2008). The use of polynomial functions to parametrically optimize the curves is a less viable possibility because they tend to make the problem non-convex, causing numerical instability. However, the use of splines proved to be an excellent alternative, especially for optimizing reinforced plates. This is because they allow the development of more complex curves while having fewer design variables (Wu, Raju, Weaver, 2015). Furthermore, through splines it is feasible to efficiently impose a minimum radius on the paths. This is important because bending radius is one of the biggest manufacturing limits for curvilinear fibers. Therefore, by restricting the path of optimized reinforcements, it is possible to guarantee that only structures that are manufacturable will be designed (Montemurro and Montemurro, Catapano, 2017).

In order to parameterize curves, Nagendra et al. (1995) first applied B-Splines as a representation of the path of reinforcements, developing the concept that was named NURBS (Non-Uniform Rational B-Spline). This modeling used non-linear optimization and was generically designed so that it could obtain the best orientation of the reinforcements in order to optimize several mechanical properties, such as vibration frequencies, strains, stresses and stiffness (Nagendra, et al., 1995). This same concept was applied in a step of Reliability-Based Design Optimization (RBDO). In this situation, the authors used the B-Splines in the lamination parameter optimization step, which aimed to reduce the weight of the experimental plates to buckling loads (Hao et al., 2021). Furthermore, another important aspect of splines is the conception of smooth and continuous curves, which maximizes the mechanical properties of structures. Thus, the use of cubic splines also demonstrated efficiency in reducing the stress concentration of plates with curvilinear reinforcements (Wu, Raju, Weaver, 2015; Hou et al., 2021).

One of the most important factors for obtaining global optima or good local optima in gradient-based optimization problems are the initial values applied to start the optimization process. There is still a large gap in terms of possible solutions to these problems. One of the large observed solution groups implements at least two algorithms in the search for an optimization solution with better computational efficiency (Xu et al, 2018). In this context, Chaparro et al. (2008) used a hybrid formulation, which started with a Genetic Algorithm (GA) followed by another gradient-based algorithm for optimizing material parameters of an aluminum alloy.

Kathiravan and Ganguli (2007) presented results of this combination of algorithms in the optimization of fibrous composites. The authors intended to obtain the optimal angles for overlapping layers of composites with straight fibers, which were used in the manufacture of blades for helicopter propellers. The initial configuration of the reinforcements was calculated by the Particle Swarm Optimization (PSO) heuristic algorithm and then a gradient-based algorithm was applied over the previously optimized structure. This process resulted in obtaining the optimal inclinations of each blade layer to maximize the Tsai–Wu–Hahn failure criterion. Kiyono et al. (2017), proposed the optimization of the angles of discretized elements by a method called Normal Distribution Fiber Optimization (NDFO), which occurs using a generic function of the normal distribution to make a previous selection of candidate discrete angles and then find the optimal angle between them. The NDFO, when confronted with previously proposed methods, was successful in improving the structural compliance and positioning of the fibers so that manufacturability is facilitated.

Although they did not propose any method for solving the problem involving the influence of the initial positions of the reinforcements on the outcome of problems involving VCS, Ding et al. (2022) warned about this aspect. According to the authors, as the VSC optimization process is highly non-convex and presents many local minima. Unlike heuristic methods, gradient methods require a primary placement of the fibers to start the optimization. As a result, it is expected that for each initial configuration a different result will be obtained. Shimoda et al. (2023) used gradient methods to simultaneously optimize the shape and density of plates and shells. The authors' objective was to seek better positioning and orientation for CFRP-type materials, which was obtained in comparison with tests proposed by them using each of the methods individually. However, even demonstrating superior performance to the implementation of only one optimization method, the authors reported that there is a dependence on the initial arrangement of the fibers to obtain the final results.

As mentioned above, there are studies that seek to solve the problem related to the initially arbitrated variables, necessary for gradient methods. However, in most cases, a solution using hybrid algorithms is proposed, which in fact

results in better final configurations, but does not seek to understand which factors interfere in the final result of the optimization. In short, the works do not aim to understand the relationship between the characteristics that make up the geometry of the filaments with the boundary conditions of the problem. In this context, Vieira, de Leon, Marczak (2022) used a variation of the initial angle of straight and continuous fibers applied in plates to observe the influence of different inclinations on the final flexibility of the structure, which was optimized by Sequential Linear Programming. In the case study, which contained three reinforcements for all observed situations, the results demonstrated a direct relationship between the initial inclination and final flexibility of the plates. It should be noted that all proposed slopes, which had the same materials and boundary conditions, were successful in the optimization, but presented very different results. In comparison between them, the difference between the best and the worst result reached approximately 280%. Therefore, the need to further investigate the relationships involving the initial arbitrariness and the results of gradient-based optimization became evident.

This work aims to deepen the investigation of the relationship between the initial placement of reinforcements and the results of gradient-based optimizations. Thus, the variation of the angle of inclination of the applied force was added to the variation of the initial angle of the straight fibers, so that the relationship between the two inclinations could be observed. Also, the influence of the number of reinforcements was also investigated, so that for each boundary condition and initial positioning between 1 and 4 filaments were used. Finally, it should be mentioned that the objective was to reduce compliance, but the maximum displacements of the structure were measured, which were related to the initial conditions and final compliance of each case study, demonstrating the influence of initial positioning and final compliance in this mechanical feature.

## 2 METHODOLOGY

Initially, the structures to be optimized will be plates containing different numbers of reinforcements. The plates are CRFPs, their matrix is epoxy resin and their reinforcements are carbon fiber. The fibers work as stiffeners. However, unlike traditional stiffeners, they are internal to the material. Material properties used throughout the cases are shown in Table 1.

**Table 1:** Properties of Materials applied in the work

Properties	Material Properties	
	Carbon Fiber	Epoxy Resin
Longitudinal Young's Modulus	230 GPa	4 GPa
Transverse Young's Modulus	15 GPa	4 GPa
Longitudinal Shear Modulus	15 GPa	1.481 GPa
Transverse Shear Modulus	7 GPa	1.481 GPa
Longitudinal Poisson's Ratio	0.2	0.35
Transverse Poisson's Ratio	0.07	0.35

The initial arrangement of the reinforcements will be straight and, for each applied force, four initial inclinations were tested. Also, the number of reinforcements on the plates is progressive, so they have 1, 2, 3 or 4 reinforcements. Furthermore, the compliance of the structure without any reinforcement was calculated and is used for comparison with the results obtained after initial implementation and optimization of carbon fibers. In this way, the results obtained are compared with each other and with the plate composed only of the matrix. Figure 1 demonstrates all the possibilities of the initial positions of the studied cases.

It is important to point out, except for the initial inclinations of the reinforcements and the directional angles of the forms, the other characteristics of the structure are always the same. Therefore, the plate is supported on two vertices, with supports that only allow rotation, without any type of translation at the structure's attachment points. Both supports are at position  $x = 0$ , one of them at point  $y = 0$  and the other at  $y = 100$  mm. The dimensions of the matrix are: 100 mm in height, 100 mm in length and 10 mm in thickness. The reinforcements have a cross-sectional area of 25 mm<sup>2</sup>. The force has a module equal to 1 kN and is always applied at the point  $x = 100$  and  $y = 50$  mm, as shown in Figure 2.

The reinforcement paths are represented by B-Splines with no intermediate control points and are in the middle plane of the plate. So, for each of the curves there are six design variables:  $x$  and  $y$  positions (initial and final) and the slope angles (initial and final) of the curve. Furthermore, when there is more than one reinforcement in the structure, they are independent of each other. Thus, they can obtain non-parallel and non-symmetric placements, according to their initial positions and boundary conditions. The optimization process is carried out through SLP, using a continuous interaction between two software: MATLAB and Ansys APDL.

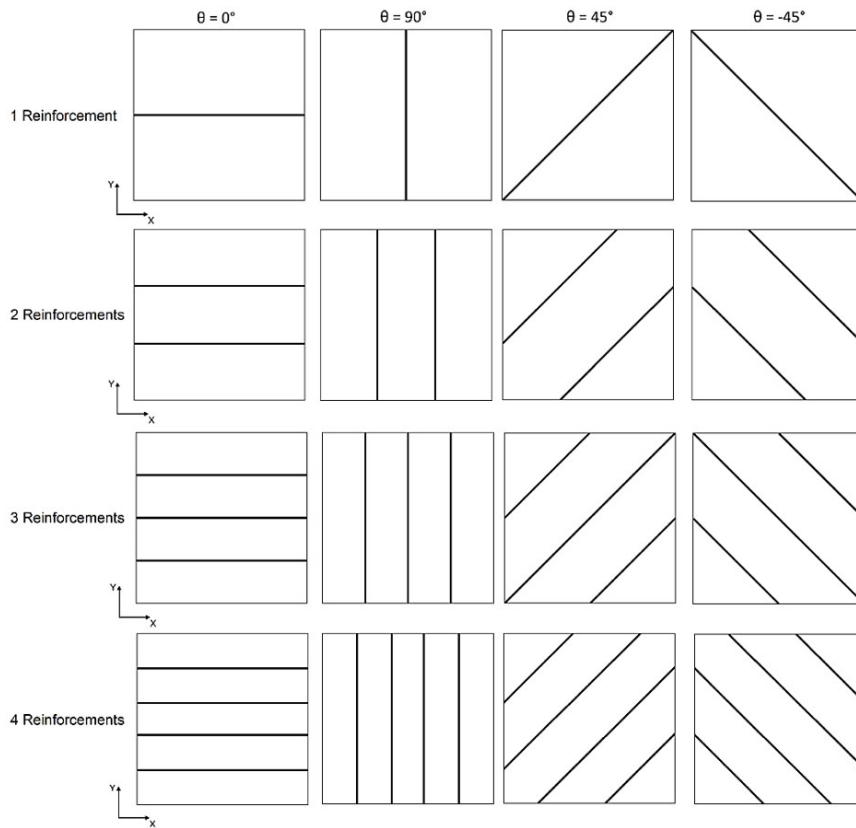


**Figure 1** Initial angle and position of the reinforcements in the cases studied

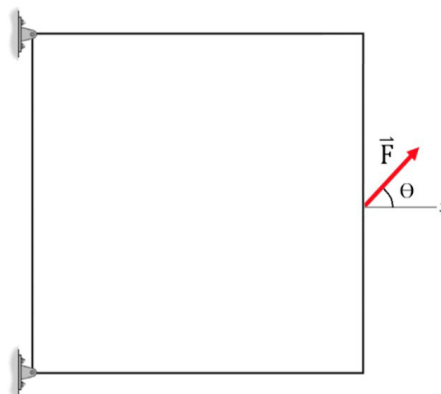


**Figure 2** Support conditions and loading

As mentioned, the modeling and optimization of the problem was done using two software's: Ansys APDL and MATLAB. In Ansys APDL the Finite Element model is built and the compliance and displacements of the structure are also calculated. In addition, it is using this software that the models implemented in the work were plotted. For modeling the problem, two types of elements are defined, a shell element (SHELL181) and a reinforcement element (REINF164). The shell model has six degrees of freedom, three integration points and its average surface was used to obtain the element properties. The reinforcement element, on the other hand, behaves identically to bar elements, has a fixed cross-sectional area and its trajectory follows the B-spline determined by the design variables, which are the values of the initial and final points and inclinations of the curve.

The mesh of the plate is established in rectangular elements containing four nodes each and edge dimensions equal to 1 mm, while the mesh of the reinforcements are rectilinear elements with the same dimension as the edge of the rectangular element. Also, a complementary element – MESH200 – is used to attach the reinforcement elements to the plate elements, without them sharing the same nodes. By solving the structure in finite elements, it is possible to obtain the compliance of the structure, which is performed by the SENE function of the software. The optimization process will be detailed in the next section.

## 2.1 Optimization Process

In order to maximize the rigidity of the structure, the optimization problem has the objective function of minimizing its compliance. This minimization is achieved by changing the angles and positions of the B-splines, according to Equation (1).

$$\begin{aligned} \min: & \mathcal{C}(x_i, y_i, \theta_i) \\ \text{subject to: } & 0 \leq x_i \leq x_{max} \\ & 0 \leq y_i \leq y_{max} \\ & 0 \leq \theta_i \leq 360^\circ \quad i = 1, 2, \dots, 2n \end{aligned} \quad (1)$$

For each fiber, two positions on the Cartesian axis  $(x_i, x_{i+1}, y_i, y_{i+1})$  and the two inclinations of the ends of the curve  $(\theta_i, \theta_{i+1})$  are used. In this situation,  $n$  represents the number of fibers applied to the plate and, therefore, each variable needs to be equal to twice the number of fibers – since there is a variable at the beginning and another at the end of each reinforcement. The limitations of the variables are established by the positions of the ends of the reinforcements on the  $x$  and  $y$  axes, which are subject to the maximum dimensions of the plates, represented by  $x_{max}$  and  $y_{max}$ . In turn, the entry and exit angles of the B-Splines have continuous variation between 0 and 360 degrees.

The process of obtaining the optimal points of the design variables is performed by SLP, which is based on Linear Programming (LP). LP is applied to problems that contain linear functions and constraints or that are linearized – which can be done using Taylor Series. Furthermore, considering the feasible domain in the optimization search space, the values obtained in the LP are located in the vertices of this domain. In this case, the values are located at the ends of the moving bounds of the variables. Linear programming can be calculated from the objective function gradient at the points and the limits for each design variable. For the optimization of the best local optimum to be feasible, it is important that the limits between the design variables are not fixed. Thus, the concept of Moving Limits is applied, that is, at each iteration there is a repositioning of the central location between the limits, which is superimposed on the optimal variable obtained in the previous iteration. So, when approaching an optimal value, the limits restrict the search space and when moving away from an optimal value, the difference between the ends of the limits is magnified. The increase or decrease of the limits is determined by the opening coefficient  $\alpha$ . This  $\alpha$  coefficient is calculated by the history of the last three results obtained, according to Equation (2).

$$\alpha = (x_{i-1} - x_{i-2})(x_{i-2} - x_{i-3}) \quad (2)$$

The expansion or reduction of the moving limits is influenced by the value of  $\alpha$ . If it is positive, it reduces the design space of the search space, whereas the negative or null value of the coefficient causes expansion between the moving limits. The dimension of these limits at each cycle is represented by  $l_i$ , which is influenced by a previously defined percentage value  $\delta$ . Equation (3) presents the behavior of the Moving Limits according to the predefined values and the results obtained in the iterations.

$$\begin{cases} l_i = (1 + \delta)l_{i-1}, & \text{if } \alpha \leq 0 \\ l_i = (1 - \delta)l_{i-1}, & \text{if } \alpha > 0 \end{cases} \quad (3)$$

Therefore, at each iteration the limits are updated according to Equation (4):

$$\begin{cases} x_{\min i} = x_i - l_i \\ x_{\max i} = x_i + l_i \end{cases} \quad (4)$$

The variables  $x_{\max i}$  e  $x_{\min i}$  are, respectively, the upper and lower limits that the variables can assume. Figure 3 demonstrates the flowchart that develops the sequence of steps implemented in the search for optimal variables.

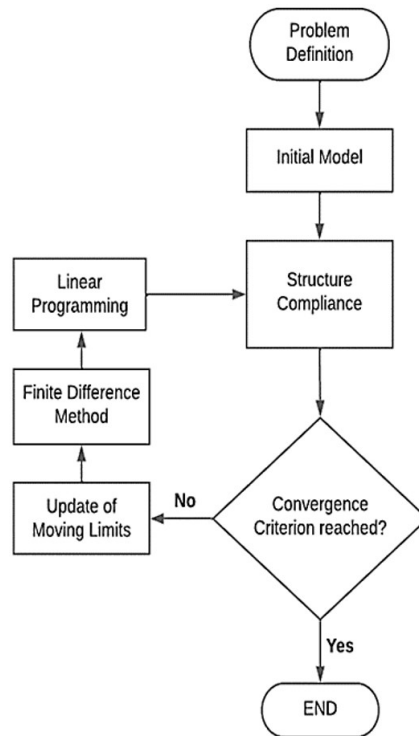


Figure 3 Structure optimization flowchart

The optimization process demonstrated in the flowchart is applied to each case study. Hence, in the “Problem Definition” step, the structure geometry, boundary conditions, process constants, number of reinforcements and their positions are defined.

After the initial compliance modeling and calculation, the algorithm enters a process cycle, which lasts until a convergence criterion is reached. The established convergence criteria are the change close to a null value of all design variables (change less than 10<sup>-6</sup>) or that 10<sup>3</sup> iterations are completed. If the convergence criteria are not reached, the moving limits are updated, according to equations (2), (3) and (4). After that, there is an infinitesimal perturbation in each design variable (Δ = 10<sup>-9</sup>) and the Finite Difference Method - which obtains the difference between the response of the variable and the response of the perturbed variable - according to Equation (5) is applied:

$$\frac{\partial f}{\partial x} \approx \frac{f(x+\Delta) - f(x)}{\Delta} \tag{5}$$

After calculating each of the design variables, a vector with the sensitivity of the elements is obtained and based on this structural response, optimization by LP is performed. This optimization is done using the LINPROG function, from MATLAB. As input data of the function, the sensitivity vectors of the elements and their respective moving limits are used. The function's output values are optimal points of the design variables in its search space. At each iteration, these optimal points are used to establish new design variables, which are used to calculate compliance. Then, there is a new verification of the convergence criterion.

### 3 RESULTS

After the insertion of reinforcements, both before and after optimization, an analysis of the mechanical behavior of the plates without reinforcements was carried out. First, the compliances were analyzed are shown in Table 2:

Table 2: Compliances of structures without reinforcements

Plates without Reinforcements	
Force (1 kN)	Compliance (Nm)
0°	0.9620
45°	1.8081
90°	2.6560

Table 2 demonstrates that loadings more parallel to the x axis result in lower compliances. By increasing the angle between the force and the x axis, a significant increase in the compliance of the structure happens, which represents a reduction in the total stiffness. Regarding the distribution of displacements, which are necessary to the calculation of the strain energy, Figure 4 shows these distributions for each of the forces applied to the structures.

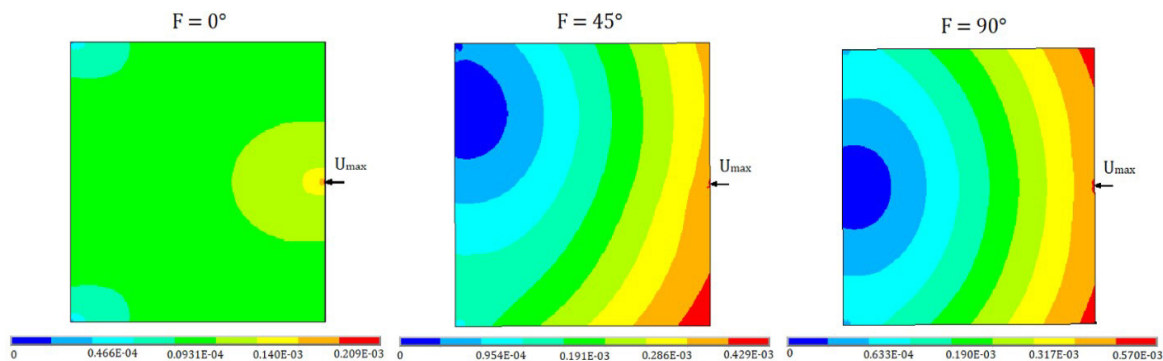


Figure 4 Displacement fields in structures without reinforcements

As noted, in all cases the maximum displacement of the structure occurs at the points where the force is applied, regardless of the slope at which it is applied. In addition, situations where there is force with angles equal to 0 and 90° show symmetry in the displacement distribution, while the same does not occur in the inclination equal to 45°. Also, there is an increase in the maximum displacement as the inclination was increased in relation to the x axis, showing 0.209E-3 mm for 0°, 0.429E-3 mm for 45° and 0.570E-3 mm for 90°.

The analysis of the strain energies, displacement and morphology of the reinforcements after the optimization process carried out in this work confirm that regardless of the boundary conditions, the initial orientation develops an influence on the final results of the process. This fact was confirmed because using the same structure, materials and boundary conditions, associated with the variation in the number of fibers, their orientation and force inclination, no identical final structure was obtained. Therefore, the following subsections will aim to individually analyze each of the structures subjected to different forces and initial inclinations of the reinforcements.

3.1 Case 1: Force = 0°

In the first case, which has a force with an inclination of 0° in relation to the x axis, the results in Table 3 show the initial and final compliance and maximum displacement for each case studied.

Table 3: Compliances and maximum displacements for 0° force

Case 1 - Force = 0°								
Compliance (Nm)								
Reinforcements	1 Reinforcement		2 Reinforcements		3 Reinforcements		4 Reinforcements	
Initial Fibers Slope Angle	Initial	Final	Initial	Final	Initial	Final	Initial	Final
0°	0.5258	0.4594	0.9045	0.0399	0.5200	0.0377	0.8640	0.0097
45°	0.7307	0.2814	0.8955	0.2154	0.5404	0.2685	0.8950	0.2683
90°	0.9303	0.9224	0.9250	0.6741	0.9214	0.4135	0.9197	0.2471
-45°	0.7307	0.3716	0.8955	0.2748	0.5404	0.2680	0.8950	0.1659
Max. Displacement (mm)								
Reinforcements	1 Reinforcement		2 Reinforcements		3 Reinforcements		4 Reinforcements	
Initial Fibers Slope Angle	Initial	Final	Initial	Final	Initial	Final	Initial	Final
0°	1.22E-04	1.15E-04	2.03E-04	1.83E-05	1.21E-04	1.68E-05	1.97E-04	8.42E-06
45°	1.85E-04	1.49E-04	2.04E-04	1.50E-04	1.77E-04	1.47E-04	2.04E-04	1.48E-04
90°	2.09E-04	2.08E-04	2.08E-04	1.87E-04	2.08E-04	1.79E-04	2.07E-04	1.47E-04
-45°	1.85E-04	1.71E-04	2.04E-04	1.51E-04	1.77E-04	1.47E-04	2.04E-04	1.43E-04

In a first observation, the compliance of the matrix is presented without the inclusion of any reinforcement, which has 0.9620 Nm. So, it is possible to see that when applying the carbon fiber, in any orientation, it naturally causes a reduction in the strain energy. However, even if it is always reduced with the implementation of reinforcements, the inclination and number of fibers used also change the initial values. The same behavior is observed in the maximum displacement, which starts with 0.209E-3 mm and except for the situation with 90° of initial inclination, there is a reduction in the dimensions of the displacement.

An important factor to be commented, based on the data obtained in Table 3, is that, the increase in the number of filaments does not always reduces compliance. This is because the curves are straight and equidistant from each other and from the ends of the plate. Therefore, it is possible to verify that the configurations with 1 and 3 reinforcements and initial inclination of 0° have the end point of the fiber coincident with the point of application of the force. This arrangement causes lower compliance rates, as this reinforcement directly supports the traction effort caused by the load. This also occurs at the 45° and -45° slopes with and reinforcements, but the strain energy is slightly higher because the load is not fully axial to the fiber.

Regarding the maximum displacements, there is a direct relationship not only between the orthogonality of the reinforcement with the force, but also the proximity of the reinforcement to the point of application of the effort. This can be proven by observing the initial placements that are parallel to the force, which have 1 and 3 filaments. In these two cases there is a point of contact between the force and the reinforcement one of the reinforcements and, even if there are situations with a greater number of reinforcements, the displacement values are greater. After optimization, this relationship does not remain the same and there is a tendency for reinforcements to approach the regions of force application. So, it should be mentioned that, although the worst results developed for each number of reinforcements are close, the largest displacement was found for the structure with only one reinforcement, which was orthogonal to the force. This result, contrary to most cases, was not close to the value of the other results, standing out negatively, since it obtained a maximum displacement equal to 2.08E-3 mm, a dimension that practically did not differ from the result before optimization, which was equal to 2.09E-3 mm. In order to graphically present the morphology resulting from the optimization of straight reinforcements with the different initial inclinations, Figure 5 presents the results obtained for the two cases with three fibers, one of them had an initial inclination of 0° and the other equal to 45°

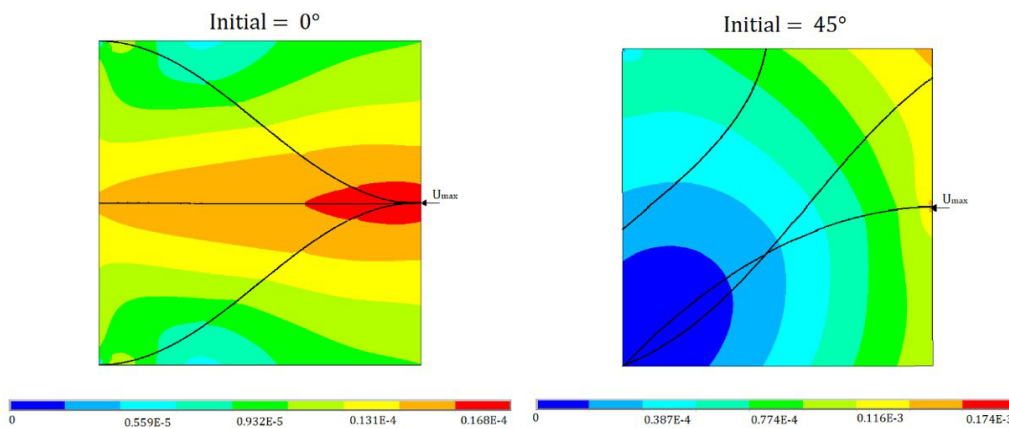


Figure 5 Distribution of displacements in structures with three reinforcement and different initial fibers slope

Another extremely important factor in the relationship between the results is to realize that, even though it is not an objective function, the maximum deformation tends to follow the percentage of compliance reduction. Table 4 presents the comparisons between the reduction of compliance and the maximum displacement.

Table 4: Displacement reduction percentages after optimization - 0° force

Case 1 - Force = 0°								
Reduction (%)	1 Reinforcement		2 Reinforcement		3 Reinforcements		4 Reinforcements	
	Compliance	Disp.(max)	Compliance	Disp.(max)	Compliance	Disp.(max)	Compliance	Disp.(max)
0°	12.63%	5.74%	95.59%	90.99%	92.75%	86.12%	98.87%	95.73%
45°	61.49%	19.46%	75.95%	26.47%	50.32%	16.95%	70.02%	27.45%
90°	0.85%	0.48%	27.13%	10.10%	55.13%	13.94%	73.13%	28.99%
-45°	49.14%	7.57%	69.31%	25.98%	50.41%	16.95%	81.47%	29.90%

As it can be seen in Table 4, there is a clear correlation with the ability to reduce compliance with the maximum displacement of structures. In general, when there is a high percentage reduction in compliance, the maximum displacement is also reduced at high levels. This becomes even clearer when we observe the cases of structures with two, three and four fibers initially with a 0° inclination, where all of them presented a percentage reduction between 92.75 and 98.87% of compliance, which resulted in a percentage reduction of maximum displacement between 86.12 and 90.99%. Reinforcing this evidence, when lower rates of compliance reduction were observed, as in the cases of structures with three reinforcements under initial inclination of 45, 90 and -45°, which had compliance reduction between 13.94 and 16.95%. Also, for a reinforcement initially at 90°, the compliance reduced by 0.85% and the maximum displacement by 0.48%. Thus, it is important to emphasize that, although there is no direct mathematical relationship that indicates a proportional percentage for the two characteristics of the structure, there is a clear correlation for them. Therefore, it is possible to infer that even if the smaller displacements along the structure are important, the compliance is very sensitive to maximum displacement changes.

### 3.2 Case 2: Force = 45°

The second case refers to structures subjected to force with an inclination of 45° in relation to the x axis. The compliances and maximum displacements are shown in Table 5:

**Table 5:** Compliances and maximum displacements for 45° force

Case 2 - Force = 45°								
Compliance (Nm)								
Reinforcements	1 Reinforcement		2 Reinforcements		3 Reinforcements		4 Reinforcements	
Initial Fibers Slope Angle	Initial	Final	Initial	Final	Initial	Final	Initial	Final
0°	1.5264	0.2762	1.6804	0.2154	1.4881	0.2044	1.6957	0.1461
45°	0.8548	0.1576	1.6099	0.1520	0.4537	0.0440	1.5861	0.1435
90°	1.7266	1.5976	1.7221	0.0637	1.7182	0.1623	1.7158	0.1427
-45°	1.6187	1.5789	1.7041	1.2240	1.6121	1.5374	1.6848	0.7309
Max. Displacement (mm)								
Reinforcements	1 Reinforcement		2 Reinforcements		3 Reinforcements		4 Reinforcements	
Initial Fibers Slope Angle	Initial	Final	Initial	Final	Initial	Final	Initial	Final
0°	4.15E-04	1.29E-04	4.23E-04	8.69E-05	4.07E-04	1.47E-04	4.13E-04	7.09E-05
45°	2.35E-04	1.24E-04	4.08E-04	1.21E-04	1.95E-04	3.60E-05	4.04E-04	1.22E-04
90°	4.26E-04	3.77E-04	4.42E-04	5.14E-05	4.28E-04	1.38E-04	4.27E-04	1.19E-04
-45°	3.86E-04	3.70E-04	4.23E-04	3.43E-04	3.85E-04	3.62E-04	4.19E-04	2.67E-04

It is possible to notice that the deformation energy in the matrix is much higher than in the previous case, in which the load is mainly traction in the plate. This strain energy is equal to 1.8081 Nm. Besides that, except for the initial inclination of 45° (coincident with the inclination of the load), there is no significant change between the strain energy of the plate without reinforcements and after the initial application of reinforcements. The only cases where there is a considerable reduction are in the 45° slopes containing one and three reinforcements. In these two initial configurations, there is coincidence of the angle of inclination of the force with the reinforcements. Furthermore, in the case with a fiber there is contact with a support point. In the case with three fibers, in addition to the contact with the support, one of the reinforcements is also directly in contact with the applied load. In turn, the worst initial result is when there is only one reinforcement and it is positioned at 90°. For the 90° inclination, the addition of rectilinear and non-optimized reinforcements causes a negligible improvement in rigidity, because there is no contact and no proximity of the supports or force. Furthermore, the force is applied at 90° from the reinforcement, which presents more relevant resistance in the axial direction.

After optimization, the case in which the greatest success was obtained was also the one with three filaments initially at 45°, in which a final compliance of 0.4537 Nm was obtained, which represents a reduction of 97.46% in relation to the matrix. It is worth noting that in all cases with an initial inclination of 45°, there was a reduction in strain energy greater than 90%. Furthermore, the implementation of four reinforcements did not improve the optimization, even developing a worse result when compare to the plate with three reinforcements.

Reinforcements started with slope equal to zero also obtained good results, which were progressive in relation to the addition of reinforcements. Thus, the plates with one, two, three and four fibers respectively obtained compliances equal to 0.2762; 0.2154; 0.2044 and 0.1462 Nm. These values represent a percentage reduction in compliance equal to 84.03; 87.65; 88.18 and 91.55%. In situations where the filaments were at an initial 90°, except with only one reinforcement, the optimization was successful in reducing compliance, obtaining 0.0637 Nm with two reinforcements, which represents a 96.32% reduction. The structures that started at an inclination of - 45° resulted in less expressive optimizations in relation to the other cases. The most representative cases of this failure were the plates with one and three reinforcements, which respectively obtained 1.5789 and 1.5374 Nm, developing only 8.72 and 11.11% of reduction in strain energy. Regardless of the number of filaments and the initial inclinations, it is evident that the best results are obtained when the reinforcements are not only on the points where efforts are applied, but they are also at the same point or very close to the point of greatest displacement. Even if there is a greater number of reinforcements, when the positioning of the fibers is in the aforementioned locations, there is a more significant reduction in compliance and maximum displacement. These statements are demonstrated in Figure 6, where we have cases with two, three and four reinforcers, but the least compliance is developed with the least number of reinforcers.

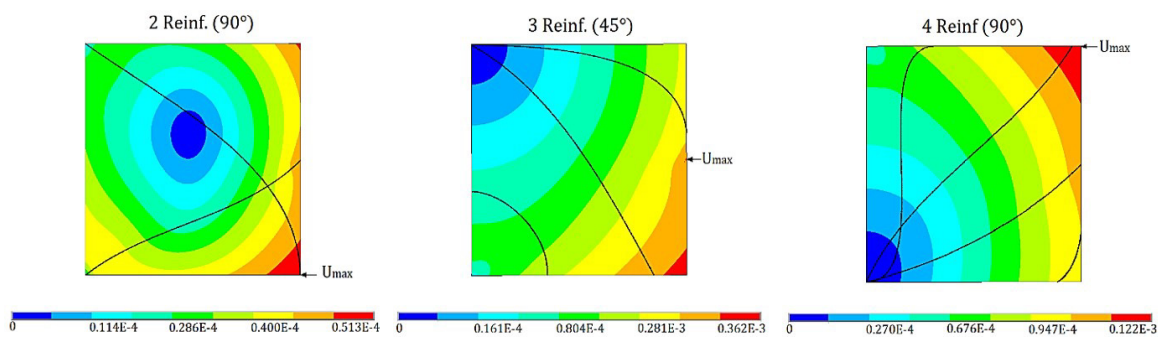


Figure 6 - Distribution of displacements in reinforcements with different number of reinforcements and initial inclination

Finally, it is also important to analyze the percentage of compliance reduction and maximum displacement of structures under 45° inclined force. Table 6 presents this information.

Table 6: Displacement reduction percentages after optimization - 45° force

Case 2 - Force = 45°								
Reduction (%)	1 Reinforcement		2 Reinforcement		3 Reinforcements		4 Reinforcements	
	Compliance	Disp. (max)	Compliance	Disp. (max)	Compliance	Disp. (max)	Compliance	Disp. (max)
0°	81.91%	68.92%	87.18%	79.46%	86.26%	63.88%	91.38%	82.83%
45°	81.56%	47.23%	90.56%	70.34%	90.30%	81.54%	90.95%	69.80%
90°	7.47%	11.50%	96.30%	88.37%	90.55%	67.76%	91.68%	72.13%
-45°	2.46%	4.15%	28.17%	18.91%	4.63%	5.97%	56.62%	36.28%

As in the first case, the correlation between the percentages of compliance reduction and maximum displacement remains. In this case, it is evident that the potential for reduced compliance and maximum displacement is very low when the fibers are orthogonal to the force. In this sense, there is an opposite effect when the angles coincide, always showing good percentages of improvements, which also occurs for the angle coinciding with the x axis. Finally, it is noticeable that the 90° angle from 2 reinforcements achieves good percentages of compliance reduction and maximum displacement.

### 3.3 Case 3: Force = 90°

Finally, in the third case, the structures with force inclined at 90° in relation to the x axis are evaluated. The values are contained in Table 7.

**Table 7:** Compliances and maximum displacements for 90° force

Case 3 - Force = 90°								
Compliance (Nm)								
Reinforcements	1 Reinforcement		2 Reinforcements		3 Reinforcements		4 Reinforcements	
Initial Fibers Slope Angle	Initial	Final	Initial	Final	Initial	Final	Initial	Final
0°	2.5270	1.2211	2.4562	0.4001	2.4562	0.0290	2.4151	0.2977
45°	1.7428	1.2678	2.4186	1.1157	1.5254	1.1113	2.3758	1.0122
90°	2.5228	1.5849	2.5193	0.5096	2.5149	0.5347	2.5120	0.0913
-45°	1.7428	1.4808	2.4186	0.2391	1.5254	1.0824	2.3758	0.2296

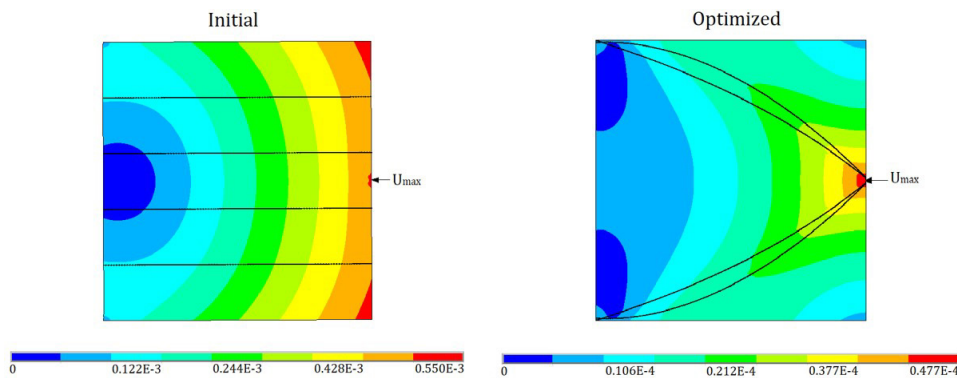
  

Max. Displacement (mm)								
Reinforcements	1 Reinforcement		2 Reinforcements		3 Reinforcements		4 Reinforcements	
Initial Fibers Slope Angle	Initial	Final	Initial	Final	Initial	Final	Initial	Final
0°	5.70E-04	3.30E-04	5.63E-04	1.25E-04	5.59E-04	3.57E-05	5.50E-04	4.77E-05
45°	4.13E-04	3.55E-04	5.22E-04	3.24E-04	4.03E-04	3.33E-04	5.45E-04	3.31E-04
90°	5.69E-04	4.48E-04	5.69E-04	1.39E-04	5.68E-04	2.91E-04	5.67E-04	2.35E-04
-45°	4.13E-04	3.64E-04	5.52E-04	7.43E-05	4.03E-04	2.36E-04	5.45E-04	7.70E-05

In the latter case, it is noticeable that the flexibility value of the plate without reinforcements is quite high compared to the previous cases, and is equal to 2.5270 Nm. In addition, the implementation of orthogonal force reinforcements (with 0° of inclination in relation to the x axis) practically do not cause reduction of compliance. However, contrary to the cases previously observed, the simple application of reinforcements straight and axially coincident with the applied force also did not cause a significant effect. This can be explained by the fact that, even with coincident inclinations, the reinforcements are far from both the supports and the force application point. In turn, the results for reinforcements with 45 and -45° inclination showed a reduction in compliance after the implementation of straight fibers. This reduction was more significant for plates with one and three reinforcements, in which there is direct contact of the filaments with the supports or with support and force, while the cases with two and four reinforcements did not show a significant reduction, neither for compliance nor for maximum displacement.

It is possible to observe, in general, the use of a single reinforcement does not cause a significant reduction in strain energy. Although the optimization has taken place, the best percentage result is 1.2211 Nm for the 0° inclination and the worst is 1.5849 Nm for the compliance to 90° inclination. For the same situations, the maximum displacements were equal to 3.30E-4 and 4.48E-4 mm. However, from the use of two reinforcements there is a significant improvement for most cases. This can also be observed in the maximum displacements, in which the inclusion of a greater number of reinforcements does not cause a reduction in this structural characteristic.

In this third case, it was possible – in addition to checking the results before and after optimization – to validate the coherence of these results. This was done by comparing it with classic results from the literature. Thus, in a first plane, the morphology of the optimized structure from the plate that initially had four reinforcements with an inclination equal to 0° was compared to the Michell Cantilever. Soon, it was confirmed that the results of the work were close to the results obtained by Michell (1904). Figure 7 shows the deformation distribution of the initial and final structure in this case.



**Figure 7** Initial and Final structures initial fiber inclination of 0°

In addition, the positioning of the reinforcements was consistent with authors who used Mitchell's structure to validate optimization algorithms based on splines. Martínez et al. (2007) used cubic splines to optimize the topology, dimensions and geometry of two-dimensional structures. Xu and Dai (2021) applied B-splines for optimization of optimized structures, which after validation through comparison with Michael's results, were extrapolated for optimization and manufacture of gears with mass reduction and optimal relationship between weight and resistance.

As in cases 1 and 2, the analysis of the reduction percentages helps in understanding the relationships between the angles of inclination of the reinforcements and the forces. Table 8 presents these results.

**Table 8:** Displacement reduction percentages after optimization - 90° force

Case 3 - Force = 90°								
Reduction (%)	1 Reinforcement		2 Reinforcement		3 Reinforcements		4 Reinforcements	
	Compliance	Disp. (max)	Compliance	Disp. (max)	Compliance	Disp. (max)	Compliance	Disp. (max)
0°	51.68%	42.11%	83.71%	77.80%	98.82%	93.61%	87.67%	91.33%
45°	27.25%	14.04%	53.87%	37.93%	27.15%	17.37%	57.40%	39.27%
90°	37.18%	21.27%	79.77%	75.57%	78.74%	48.77%	96.37%	58.55%
-45°	15.03%	11.86%	90.11%	86.54%	29.04%	41.44%	90.34%	85.87%

Analyzing the case where the initial inclination is 45°, we noticed that even three reinforcements do not result in a very effective optimization of the structure. By including a fourth carbon fiber, although still less effective than the other inclinations observed, it was possible to obtain compliance of 1.0122 Nm, reducing the percentual for 39.27%. The case that started with -45° showed an oscillation as reinforcements were added. Like the others, with one reinforcement, it obtained a low optimization, but with two reinforcements, it reached 0.2418 Nm initial and 1.1157 Nm in the final compliance, which is equal to 50.87% reduction. The behavior in relation to the maximum initial displacement is similar, for the initial straight filaments there is an increase of 0.413E-4 mm 0.522E-4 mm. After optimization, the results are very close and both obtained reductions, which were equal to 14.04% and 37.93%, respectively for one and two reinforcements. However, when adding the third filament, it again obtained a less expressive reduction, which was improved with the addition of the fourth fiber. Contrary to the situation prior to the optimization process, the reinforcements with 0° and 90° of initial inclination were the ones that obtained the best final results.

The 90° cases developed very similar final strain energy values for both two and three reinforcements. By including the fourth reinforcement, 0.0913 Nm was obtained, equivalent to a 96.37% reduction in compliance and 58.55% for maximum displacement. Finally, the case with 0° orientation achieved the best result for structures with strength at a 90° angle, which occurred with three reinforcements, in which the final compliance was 0.0290 Nm maximum displacement equal to 5.57E-5 mm, a reduction of 98.82% in relation to the initial compliance and 93.61% to the initial displacement. By adding one more filament, the percentual performance of the structure decreased, causing a smaller reduction, equal to 87.67% and 91.33%, respectively for compliance and maximum displacement.

## 4 CONCLUSION

From the analysis of the results obtained in the work, it is possible to conclude that there is a significant change in compliance before and after optimization according to the initial configuration of the reinforcements. Thus, the observations made in this study contribute significantly to the literature that is still little explored, which relates the initial positioning with obtaining better local optimum in fiber-reinforced plates. Therefore, among all the points observed, the most important ones will be highlighted below:

- There is no direct relationship between low initial compliance and better final results. As observed in the examples, the plates with the lowest compliances before optimization were not the ones that presented the lowest compliances after the process.
- The slope of the reinforcements is not an isolated factor for obtaining the best results. The coincidence of the slope of the force with the reinforcements does not guarantee that the best local optima are reached. While in most cases it is an important factor, just aligning the load with the filament is not enough to achieve the greatest reductions in compliance.
- Although reducing maximum displacement is not an objective function, in general, the best results for compliance reduction also reduce the maximum deformation developed in the structure.

- In most cases, the angular alignment of the initial fiber with the force promotes the best results in reducing compliance, this occurred with the forces applied at 0 and 45°, respectively 0.0097 and 0.0440 Nm. However, in the force applied at 90°, the best result was obtained with fibers with an inclination of 0°, which was equal to 0.0290 Nm and the best result starting with fibers at 90° was 0.0913 Nm, which can be considered a good result compared to most final compliances, but not the best.
- The smallest displacements were obtained following the same compliance logic. The 0 and 45° inclinations developed the best results when they were applied to fibers with the same force inclination, obtaining, respectively, 0.168E-5 and 3.60E-5 mm. As for the 90° inclination of the fibers, the best result was obtained with the force at 0°, which was equal to 4.77E-5 mm.
- The inclusion of a greater number of reinforcements does not imply a reduction in compliance. In the case of force at 0°, the lowest compliance – equal to 0.0097 Nm – was obtained with four reinforcements. For force equal to 45 and 90°, the lowest compliance was obtained with 3 reinforcements, and the values were equal to 0.0440 Nm and 0.0290 Nm.
- There was also a variation in the number of reinforcements to obtain the smallest displacements. While the cases started with fibers inclined at 45 and 90° showed the smallest maximum displacements – respectively 3.6E-5 and 3.57E-4 mm - when they had three reinforcements, the smallest displacement values were obtained when four were implemented. reinforcements, reaching a value equal to 8.42E-6 mm.
- Observing the relationship between better results, both for compliance and for maximum displacement, it is possible to conclude that there is a limit in the insertion of reinforcements. This limit is particular to each case and, when inserting more reinforcements than necessary, there is no improvement in the structure properties and a drop in performance begins to occur.
- A factor observed in the best results was the coincidence of the ends of the reinforcements with the support points or load application points or at least a proximity to these points.

According to the facts presented, the importance of expanding studies on the subject is evident. One of the factors to be studied in the near future is to quantitatively evaluate the influence of the distance between reinforcements and supports and forces. Thus, together with the angle of inclination of the filaments, to elaborate a more assertive method for the initial positioning of the reinforcements, aiming at the best results after optimization.

**Author's Contributions:** Vieira, E.R.: literature review, paper elaboration, algorithm development, simulations, writing. de Leon, D. M.: development of optimization strategies, review, advising. Marczak, R. J.: elaboration of the methodology, advising, review.

**Editor:** Marco L. Bittencourt and Josué Labaki

## References

- Abdalla, M. M.; Gürdal, Z.; Abdelal, G. F. (2009). Thermomechanical response of variable stiffness composite panels. *Journal of Thermal Stresses*. 32:187–208.
- Albazzan, M. A. et al. (2019). Efficient design optimization of nonconventional laminated composites using lamination parameters: A state of the art. *Composite Structures*. 209:362–374.
- Aragh, S. B. et al., (2021). Manufacturable insight into modelling and design considerations in fibre-steered composite laminates: State of the art and perspective. *Computer Methods in Applied Mechanics and Engineering*, 379:1137-1152.
- Arora, S. J., (2016). *Introduction to Optimum Design*, Elsevier Inc.
- Bai, J. (2013). *Advanced fibre-reinforced polymer (FRP) composites for structural applications*. Woodhead Publishing Limited.
- Brooks, T.R., Martins, J.R.R.A., (2018). On manufacturing constraints for tow-steered composite design optimization., *Composite Structures*, 204: 548–559.
- Chaparro, B. M. et al. (2008). Material parameters identification: Gradient-based, genetic and hybrid optimization algorithms. *Computational Materials Science*. 44: 339-346.

- Das, M., Sahu, S., Parhi, D. R. (2021) Composite materials and their damage detection using ai techniques for aerospace application: A brief review. *Materials Today: Proceedings*. 44:955–960.
- Ding, S. et al. (2022). Simultaneously optimized healing efficiency and mechanical strength in polymer composites reinforced by ultrahigh loading fillers based on interfacial energy and dynamic disulfide bonds. *Polymer*. 251:711-779.
- Gürdal, Z.; Olmedo, R. (1993). In-plane response of laminates with spatially varying fiber orientations: Variable stiffness concept. *AIAA Journal*. 31:751–758.
- Gürdal, Z.; Tatting, B. F.; Wu, C. K. (2008) Variable stiffness composite panels: Effects of stiffness variation on the in-plane and buckling response. *Composites Part A: Applied Science and Manufacturing*. 39:911–922.
- Hao, P. et al. (2021). Efficient reliability-based design optimization of composites structures via isogeometric analysis. *Reliability Engineering and System Safety*. 209:17465-17478.
- Hou, Z. et al., (2021). Optimization design and 3D printing of curvilinear fiber reinforced variable stiffness composites. *Composites Science and Technology*. 201:1085-1102.
- Jiang, C.; Han, X.; Liu, G. P. (2008). Uncertain optimization of composite laminated plates using a nonlinear interval number programming method. *Computers and Structures*. 86:1696–1703.
- Kathiravan, R.; Ganguli, R. (2007) Strength design of composite beam using gradient and particle swarm optimization. *Composite Structures*. 81:471-479.
- Kesarwani, S. (2017). Polymer Composites in Aviation Sector. *International Journal of Engineering Research*. 6:260-291.
- Kiyono, C.Y; Silva, E.C.N; Reddy, J.N. (2017) A novel fiber optimization method based on normal distribution function with continuously varying fiber path. *Composite Structures*. 160:503-515.
- Kochenderfer, M. J., Wheeler, T. A. (2019). *Algorithms for Optimization*. MIT Press.
- Martínez, P.; Martí, P.; Querin, O. M. (2007). Growth method for size, topology, and geometry optimization of truss structures. *Structural and Multidisciplinary Optimization*. 33:13–26.
- Meng, L. et al. (2020). From Topology Optimization Design to Additive Manufacturing: Today's Success and Tomorrow's Roadmap. *Archives of Computational Methods in Engineering*. 27:805–830.
- Michell, A.G.M. (1904). The limit of economy of material in frame structures. *Philosophical Magazine*. 8:589-597.
- Monte, S. M. C. et al. (2017). Optimization of fibers orientation in a composite specimen. *Mechanics of Advanced Materials and Structures*. 24:410–416.
- Montemurro, M.; Catapano, A. (2017). On the effective integration of manufacturability constraints within the multiscale methodology for designing variable angle-tow laminates. *Composite Structures*. 161:145-159.
- Nagendra, S. et al. (1995). Optimization of Tow Fiber Paths for Composite Design. *Structures, Structural Dynamics and Materials Conference*.
- Nikbakt, S., Kamarian, S.; Shakeri, M., (2018). A review on optimization of composite structures Part I: Laminated composites. *Composite Structures*. 195:158–185.
- Nocedal, J., Wright, S. J. (2006). *Numerical optimization*, Springer.
- Punera, D.; Mukherjee, P. (2022). Recent developments in manufacturing, mechanics, and design optimization of variable stiffness composites. *Journal of Reinforced Plastics and Composites*. 41:917-945.
- Rana, S.; Figueiro, R. (2016). *Advanced composites in aerospace engineering*. Elsevier.
- Shimoda, M. et al. (2023). Shape and topology optimization method for fiber placement design of CFRP plate and shell structures. *Composite Structures*. 309:116729.
- Van Tooren, M. J. L.; Elham, A. (2016). Optimization of variable stiffness composite plates with cut-outs subjected to compression, tension and shear using an adjoint formulation. *57th AIAA/ASCE/AHS/ASC Structures, Structural Dynamics, and Materials Conference*. San Diego, EUA. 1–15.
- Vasiliev, V. V; Morozov, E. V. (2007) *Advanced Mechanics of Composite Materials*. Elsevier Ltd.

- Vieira, E. R.; de Leon, D. M.; Marczak, R. J. (2022). Influence of Reinforcement Initial Positions in Optimization on CRFP Plates. Proceedings of the 8th International Symposium on Solid Mechanics. São Paulo, Brazil.
- Xu, G.; Dai, N. (2021). Michell truss design for lightweight gear bodies. *Mathematical Biosciences and Engineering*. 18:1653–1669.
- Xu, Y. et al. (2018). A Review on the Design of Laminated Composite Structures: Constant and Variable Stiffness Design and Topology Optimization. *Advanced Composites and Hybrid Materials*. 1:460–477.
- Wu, Z., Raju, G., Weaver, P.M., (2015). Framework for the buckling optimization of variable-angle tow composite plates. *AIAA Journal*. 53:3788–3804
- Wu, Z.; Raju, G.; Weaver, P.M. (2018) Optimization of postbuckling behavior of variable thickness composite panels with variable angle tows: Towards “Bucle-Free” design concept. *International Journal of Solids and Structures*. 251:66-79.